TWO-DIMENSIONAL CU-WATER NANOFLUID FLOW AND HEAT TRANSFER OVER AN INCLINED WALL AND BETWEEN TWO INCLINED WALLS: THE NUMERICAL SOLUTION OF PDES AND ODES

Mohammadreza AZIMI, Shidvash VAKILIPOUR [*]

[*]Faculty of New Sciences and Technologies, University of Tehran, Tehran, Iran.

[*] Corresponding author; E-mail: vakilipour@ut.ac.ir

In this paper, we attempt to investigate the steady and laminar flow of incompressible Water based nanofluid between inclined plates and over an inclined plate. A uniform and external magnetic field is applied in order to control the nonfluid flow. Copper-Water based nanofluid can be also used for heat transfer enhancement. We can gain additional thermal energy in the fluid by increasing the volume fraction of copper nanoparticles in the base fluid and improving the thermophysical parameters for the single-phase model. The results also show that adjusting the Prandtl and Eckert numbers causes the velocity profile to change fast. According to our findings, fluid elements may be more intensively accelerated by raising the nano additive concentration and enhancing the thermo-physical characteristics of the fluid.

Key words*: Heat Transfer; Nanofluid; Nonparallel walls; Inclined Walls; Nanofluid Flow.*

Nomenclature			
B_0	Magnetic field(wb.m^{-2})	θ	Any angle
$F(\eta)$	Dimensionless velocity	ρ	Density
Ha	Hartmann number	φ	Nanoparticle volume fraction
M	Magnetic Parameter	μ	Dynamic viscosity
P	Pressure term	ν	Kinematic viscosity
Re	Reynolds number	β	Constant
r, θ	Cylindrical coordinates	***Subscripts***	
V	Velocity vector	∞	Condition at infinity
u, v	Velocity components along x, y axes, respectively	Nanofluid	*nf*
Greek symbols		Base fluid	f
α	Angle of the channel	s	Nano-solid-particles
η	Dimensionless angle		

1. Introduction

Nanomaterials' superior thermal properties enable for more efficient heat transmission in engineering, industrial, and technological operations. By altering the concentration of the nanoparticles, the characteristics of nanofluids may be adjusted [1]. Sheikholeslami et al [2] investigated the six-lobed absorber tube with integrated turbulators. To boost the solar unit's productivity, the authors mixed Hybrid nanoparticles into the base fluid. A visualization experiment was carried out by Zhang et al [3] using a high-speed for enhancing the heat transfer performance of pulsating heat pipe. The influence of varied concentrations of SiO2-H2O nanofluid on the thermal performance of pulsing heat pipes was explored experimentally. Olabi et al [4] examined the use of nanofluids in heat exchangers of various shapes. The use of nanofluids was shown to increase heat transfer both experimentally and statistically. The thermal performance of a small heat sink thermoelectric cooling module using water-based nanofluid is explored experimentally in a work by Wiriyasart et al [5]. Azimi and Riazi [6] investigated a situation of nanofluid flow between two spinning disks for unstable nanofluid flows.

Azimi and Mozzafari [7] exploited an intelligent black-box identifier to study the unsteady 2D Graphene Oxide-water nanofluid heat transfer between two infinite parallel walls. Wire drawing, Extrusion, hot rolling, and other applications such as metal spinning, rely on fluid flow across a stretched surface [8]. To ensure that the end product fulfils the specified quality criteria, it is critical to understand the process's flow and heat characteristics [9]. With both non-Newtonian and Newtonian fluids, as well as applied electric and magnetic fields, variable thermal boundary conditions, and power law change of the stretching velocity, a wide range of issues involving heat and fluid flow across a stretching sheet have been explored. The convective transport equations are discussed in terms of similarity as well as direct numerical solutions. In this paper our hypothesizes are as follows: Addition of nanoparticles can increase the heat transfer coefficient in the system. The volume fraction parameter of nanoparticles (copper) can play an important role in how the temperature profile is formed, and in particular, the addition of nanoparticles increases the heat transfer rate.

Today, the issue of increasing heat transfer rate is one of the most important issues in industrialization. In industrial applications, especially pure water is used as a cooling fluid and ethylene glycol and oil, which due to low thermal conductivity, there is a need to increase the heat transfer rate. For this reason, nanofluids can be used for cooling, which can increase the heat transfer rate by improving the thermophysical properties of the base fluid [10].

The majority of problems in fluid mechanics including viscous nanofluid flow over a stretching wall and or between two inclined walls are nonlinear in nature and are characterized by nonlinear differential equations.Consequently, these equations are usually solved using numerical and analytical methods such as the Hermite wavelet method (HWM) [11], Homotopy Perturbation Method (HPM) [12], Reconstruction of Variational Iteration Method (RVIM) [13], and Galerkin Optimal Homotopy Asymptotic Method (GOHAM) [14]. In this paper, we presented the results of the numerical solutions for nanofluid flow between two inclined walls and over an inclined wall.

2. Related works

The topic of nanofluid flow and heat transmission over a stretched surface has piqued the interest of many academics in recent years[15-18]. Al-Mamun et al. [19] considered non-Newtonian

nanofluids flow over the stretching sheet in similar conditions. In this work, the effects of viscous dissipation and natural convection have not been investigated. The authors report that the velocity profile increases with increasing caisson fluid parameter. The similarity solution was performed to convert the equations and then the ordinary differential equation was solved with MATLAB. In an article by Khashi'ie et al [20] the effect of using hybrid nanofluid on the velocity profile in the problem of 3D fluid flow over the elastic sheet was discussed. They have obtained the results assuming a single-phase model. In this paper, the effect of viscosity dissipation is considered negligible. There is no information regarding the behaviour of velocity profiles before and after imposing external magnetic field.

Wahid et al. [21] investigated the flow of nanofluid over an elastic plate by considering the slip conditions on the wall. They have studied the impact of several parameters on temperature and velocity profiles. They reported that as the volume fraction of copper nanoparticles in the base fluid increases, the local Nusselt number on the wall increases. In this article, similarity solution was used. Ali et al. [22] investigated the effect of magnetic dipole on the heat transfer phenomenon for the ethylene glycol based nanofluid containing ferromagnetic nanoparticles. They have presented the solution results of the nanofluid flow problem over a stretching sheet. The applied magnetic field has a special effect on the nanoparticles and the fluid flow can be controlled with the help of the applied magnetic field. The finite element method has been used to solve ordinary nonlinear differential equations. According to the results obtained by the authors of this paper, ferromagnetic nanoparticles have the potential to achieve higher heat transfer compared to free magnetic nanoparticles.

Hazarika et al. [23] considered the effect of a magnetic field on a water-based nanofluid flow as it passed over an elastic plate. Viscous dissipation effect is taken into account but the natural convection coefficient is assumed to be very low. According to the results, increment of nanoparticles solid volume fraction decreases dimensionless velocity. The effect of magnetic field on the flow of non-Newtonian fluid in the presence of nanoparticles has been investigated in a paper by Hayat et al [24]. This article considers a 2D incompressible viscous MHD copper-water nanofluid flow over an inclined stretching wall and between two inclined walls.Specific instructions

3. Problem Description

3.1. Case. A:

Here, we consider the steady 2D flow of an incompressible water based nanofluid fluid between two inclined and rigid walls. The semi angle between the electrically isolated plates is fixed by the angle of 2α. The regime is laminar. We have assumed that the rigid non-parallel plates meeting at a vertex, with sink or source at the mentioned vertex, are extended to infinity. In order to investigate Jeffery-Hamel problem, a homogeneous external magnetic field which is applied in z-direction, is considered in this work. The working water-based nanofluid is electrically conducting fluid and it contains Cupper nanoparticles.

A polar coordinate system with its origin at the apex is defined for formulating the Jeffery-Hamel problem. A homogenous magnetic field (the strength is B) is applied externally on the working water-based nanofluid in the transverse direction. This magnetic field can produce a body force called Lorentz force and it is possible for us to control the fluid flow by changing the strength of the applied magnetic field. It is very important to note that the flow is purely radial. By assuming a purely radial flow in the defined polar coordinates, the problem will be simplified and similarity solution

transformation can be derived. As the flow is purely radial, there is just one velocity component (v_r) and this velocity component is a function of radial and angular coordinates (under steady state conditions). However, according to the previous research works, this important assumption can be violated even for a Newtonian fluid [25, 26].

The governing equations of MHD water-cupper nanofluid flow in a wedge-shaped channel with a fixed angle, can be written as follows (The fluid is incompressible, the flow is purely radial, steady and laminar):

$$\frac{\rho_{nf}}{r}\frac{\partial\left(ru(r,\theta)\right)}{\partial r}=0 \tag{1}$$

$$\begin{aligned} u(r,\theta)\frac{\partial u(r,\theta)}{\partial r} &= -\frac{1}{\rho_{nf}}\frac{\partial P}{\partial r}+v_{nf}\left(\frac{\partial^2 u(r,\theta)}{\partial r^2}+\frac{1}{r}\frac{\partial u(r,\theta)}{\partial r}+\frac{1}{r^2}\frac{\partial^2 u(r,\theta)}{\partial \theta^2}-\frac{u(r,\theta)}{r^2}\right) \\ &\quad -\frac{\sigma B_0^2}{\rho_{nf} r^2}u(r,\theta) \end{aligned} \tag{2}$$

$$-\frac{1}{\rho_{nf} r}\frac{\partial P}{\partial \theta}+\frac{2\mu_{nf}}{\rho_{nf} r^2}\frac{\partial u(r,\theta)}{\partial \theta}=0 \tag{3}$$

The Energy and concentration equations can be also written as follows :

$$\begin{aligned} u(r,\theta)\frac{\partial T(r,\theta)}{\partial r} &= \alpha_{nf}\left(\frac{\partial^2 T(r,\theta)}{\partial r^2}+\frac{1}{r}\frac{\partial T(r,\theta)}{\partial r}+\frac{1}{r^2}\frac{\partial^2 T(r,\theta)}{\partial \theta^2}\right) \\ &\quad +\frac{\mu_{nf}}{\left(\rho C_p\right)_{nf}}\left(4\left(\frac{\partial u(r,\theta)}{\partial r}\right)^2+\frac{1}{r^2}\left(\frac{\partial u(r,\theta)}{\partial \theta}\right)^2\right) \\ &\quad +\frac{DK_T}{C_s\left(\rho C_p\right)_{nf}}\left(\frac{\partial^2 C(r,\theta)}{\partial r^2}+\frac{1}{r}\frac{\partial C(r,\theta)}{\partial r}+\frac{1}{r^2}\frac{\partial^2 C(r,\theta)}{\partial \theta^2}\right) \end{aligned} \tag{4}$$

$$\begin{aligned} u(r,\theta)\frac{\partial C(r,\theta)}{\partial r} &= D\left(\frac{\partial^2 C(r,\theta)}{\partial r^2}+\frac{1}{r}\frac{\partial C(r,\theta)}{\partial r}+\frac{1}{r^2}\frac{\partial^2 C(r,\theta)}{\partial \theta^2}\right) \\ &\quad +\frac{K_T D_T}{T_m}\left(\frac{\partial^2 T(r,\theta)}{\partial r^2}+\frac{1}{r}\frac{\partial T(r,\theta)}{\partial r}+\frac{1}{r^2}\frac{\partial^2 T(r,\theta)}{\partial \theta^2}\right)-K_1 C \end{aligned} \tag{5}$$

Subject to the following boundary conditions:

$$\theta = 0 \ \rightarrow u_r = U, \frac{\partial u(r,\theta)}{\partial \theta} = 0, \frac{\partial T(r,\theta)}{\partial \theta} = 0, \frac{\partial C(r,\theta)}{\partial \theta} = 0 \quad \textbf{(6)}$$

$$\theta = \propto \rightarrow u = 0, T = T_w, C = C_w$$

Here θ and r are the polar coordinate system's components, $u(r,\theta)$ is velocity component in r-direction, and it is assumed to be a function of θ and r. In the aforementioned equations, P is the pressure, B_0 is the strength of the imposed magnetic field, ρ_{nf} is the density of nanofluid while v_{nf} is the kinematic viscosity coefficient.

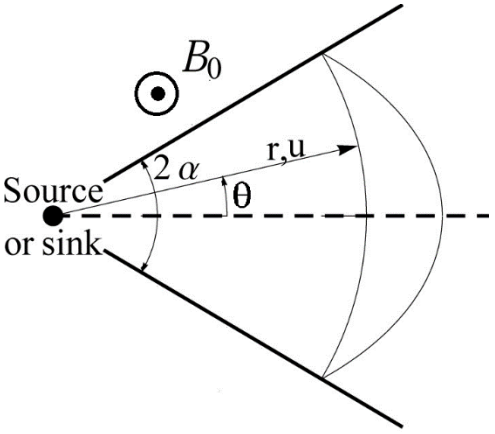

Fig. 1. Geometry of problem – Case A.

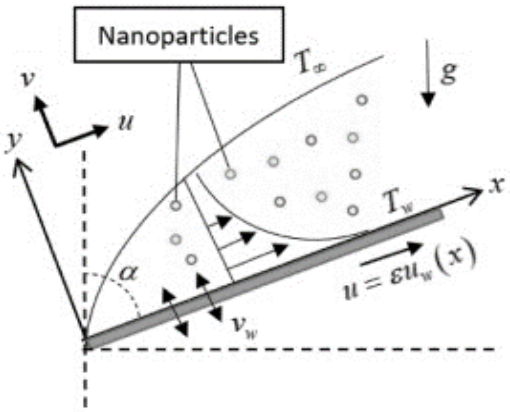

Fig. 2. Geometry of problem – Case B.

As it is depicted in Fig.1 and due to the fact, that at the walls, the nanofluid has zero velocity (the no-slip condition) the boundary conditions can be defined. We can assume that $u(r,\theta) = 0$ at the plates while at the centreline between the walls $\frac{\partial u(r,\theta)}{\partial \theta} = 0$ is assumed (according to the rule of symmetry). The working nanofluid is a water based nanofluid and its solid volume fraction is φ. The physical properties (such as density and the kinematic viscosity [6]) and thermal properties (such as thermal conductivity [7] of the nanofluid can be defined as follows:

$$\begin{cases} \rho_{nf} = \rho_f(1-\phi) + \rho_s\phi \\ \mu_{nf} = \dfrac{\mu_f}{(1-\phi)^{2.5}} \\ v_{nf} = \dfrac{\mu_f}{\rho_{nf}} \\ \alpha_{nf} = \dfrac{k_{nf}}{(\rho C_p)_{nf}} \\ \dfrac{k_{nf}}{k_f} = \dfrac{(k_s + 2k_f) - 2\phi(k_s - k_f)}{(k_s + 2k_f) + \phi(k_s - k_f)} \end{cases} \quad \textbf{(7)}$$

Introducing $\eta = \frac{\theta}{\alpha}$ and $f(\theta) = ru(r,\theta)$ the velocity parameters dimensionless form can be obtained by dividing to its maximum values ($F(\eta) = \frac{f(\theta)}{f_{max}}$) .

Substituting the introduced dimensionless parameters into Eqs.(3-6) and also eliminating the pressure term achieves the following ordinary differential equation:

$$F''' + 2\alpha Re(1-\varphi)^{2.5}\left[\frac{\rho_s}{\rho_f}\varphi + (1-\varphi)\right]FF' + (4 - H(1-\varphi)^{1.25})\alpha^2 F' = 0 \quad \textbf{(8)}$$

Where φ is the solid volume fraction of cupper nanoparticles. H and Re are Hartman and Reynolds numbers respectively. The boundary conditions can be also rewritten:

$$F(1) = 0, \quad F(0) = 1, \quad , F'(0) = 0 \tag{9}$$

The coefficient of kinematic viscosity of the working nanofluid should be measured using the predetermined formula in Eq.(7).
The achieved Eq.(8) is a nonlinear differential equation and classical techniques cannot solve this problem. Hence, we have chosen Runge Kutta method for solving the equation and also, we have solved the equation analytically in order to be sure about the accuracy of the achieved results.

3.2. **Case B:**

Consider the two-dimensional nanofluid flow on an inclined elastic wall. The sheet is being linearly stretched with constant speed of $U_w(x) = cx$ where c is a positive and constant parameter. A permanent and constant magnetic field B_0 is continuously applied in the y direction. Considering Cartesian coordinates, we write the equations of mass, momentum and energy for the proposed problem:

$$\frac{\partial u}{\partial x} + \frac{\partial v}{\partial y} = 0 \tag{10}$$

$$u\frac{\partial u}{\partial x} + v\frac{\partial v}{\partial y} = v_{nf}\frac{\partial^2 u}{\partial y^2} + g\frac{(\rho\beta)_{nf}}{\rho_{nf}}(T - T_\infty)cos\alpha - \frac{\sigma_e B_0^2}{\rho}u \tag{11}$$

$$u\frac{\partial T}{\partial x} + v\frac{\partial T}{\partial y} = \propto_{nf}\frac{\partial^2 T}{\partial y^2} + \left(\frac{\mu}{\rho cp}\right)_{nf}\left(\frac{\partial u}{\partial y}\right)^2 \tag{12}$$

The schematic of the problem can be seen in Fig.2. Here, ϕ is nanoparticles solid volume fraction. According to Fig.2, on the stretching wall we have $T_w = T_\infty + ax^2$ where a is a positive constant parameter. In light of the mentioned conditions and the assumptions of the problem, we can express the boundary conditions:

$$u = U_w, v = v_w(y), T = T_w(x) \ \ at \ \ y = 0 \tag{13}$$

$$u \to 0, T \to 0 \ at \ y \to \infty$$

It should be noted that $v_w(y)$ is the suction velocity at the porous stretching sheet. We define the following parameters for nondimensionalization of the partial differential equations:

$$\eta = \left(\frac{c}{\nu_f}\right)^{0.5} y, \psi = \left(c\nu_f\right)^{0.5} xf(\eta), u = \frac{\partial \psi}{\partial y}, v = -\frac{\partial \psi}{\partial x} \tag{14}$$

$$\theta(\eta) = \frac{T - T_\infty}{T_w - T_\infty}$$

The non-dimensional form of the resultant equations, as well as accompanying boundary conditions, can be stated by substitution of Eq.(14) in Eq.(10-12):

$$\frac{1}{FG}f''' + ff'' - f'^2 - \frac{1}{G}Mf' + \frac{H}{G}\lambda\theta = 0 \quad \textbf{(15)}$$

$$\frac{K}{PrJ}\theta'' + f\theta' + \frac{1}{FJ}Ecf''^2 - 2f'\theta = 0$$

$$F = (1-\phi)^{2.5}, \qquad G = (1-\phi) + \frac{\rho_s}{\rho_f}\phi \quad , H = (1-\phi) + \frac{\beta\rho_s}{\beta\rho_f}\phi$$

$$K = \frac{(1-\phi) + 2\phi\left(\frac{k_s}{k_s - k_f}\right) ln\left(\frac{k_s + k_f}{2k_f}\right)}{(1-\phi) + 2\phi\left(\frac{k_f}{k_s - k_f}\right) ln\left(\frac{k_s + k_f}{2k_f}\right)}, \quad J = (1-\phi) + \frac{C\rho_s}{C\rho_f}\phi$$

With the following boundary conditions:

$$f = S, f' = 1, \theta = 1, as\ \eta = 0 \quad \textbf{(16)}$$

$$f' \to 0, \theta \to 0, as\ \eta \to \infty$$

Where:

$$M = \frac{\sigma_e B_0^2}{\rho c}, \lambda = \frac{g\beta x}{u_w^2}(T_w - T_\infty), Pr = \frac{\nu f}{\alpha f}, Ec = \frac{u_w^2}{Cp(T_w - T_\infty)}, S = -\frac{vw}{\sqrt{cvf}} \quad \textbf{(17)}$$

4. Results and Discussions

4.1. Case A:

In the first part, magnetohydrodynamic nanofluid flow of an electrically conducting water-based nanofluid between two inclined walls is investigated and studied analytically and numerically. This theoretical study has many industrial applications like controlling of flows and/or design of diagnostic devices which make use of the tissue fluids and magnetic fields interaction.This paper presents an approximate solution for MHD flows of nanofluid between two rigid inclined isolated walls. The mass, momentum, energy and concentration conservation equations were presented and studied. However, the main goal of this article is to discuss about the effects of different physical parameters on the velocity profile.

It is also worth mentioning that while application of magnetic field can produce Lorentz force and it gives us this possibility to control the flow , adding copper nanoparticles to the base fluid leads to enhancement of the heat rate. Copper has higher thermal conductivity in comparison with base fluid (water) so dispersion of nanoparticles in water can hugely improve the thermal properties of the working fluid. For both cases diverging and converging channel (the negative and positive values of fixed angle between the inclined walls), the channel angle effect of velocity profile is shown in Fig.3.a,b. It is worth mentioning that for achieving both figures we assumed Re = 30, φ =0.1 and H=100.

It can be concluded that while the velocity is a decreasing function of channel angle in diverging channel, we can expect an increment in the dimensionless velocity when channel angle increases in convergent channel. This is due to the fact that in diverging channels an increase in the angle between the rigid walls may accelerate fluid elements near the plate. This may lead to an increase in the amount

of the positive pressure gradient. Hence, in a diverging channel by increasing the channel angle to a certain value, a backflow will occur. Fig.4, shows the effect Hartman number (representative of magnetic force) on velocity profile for a diverging channel (positive half-angle).

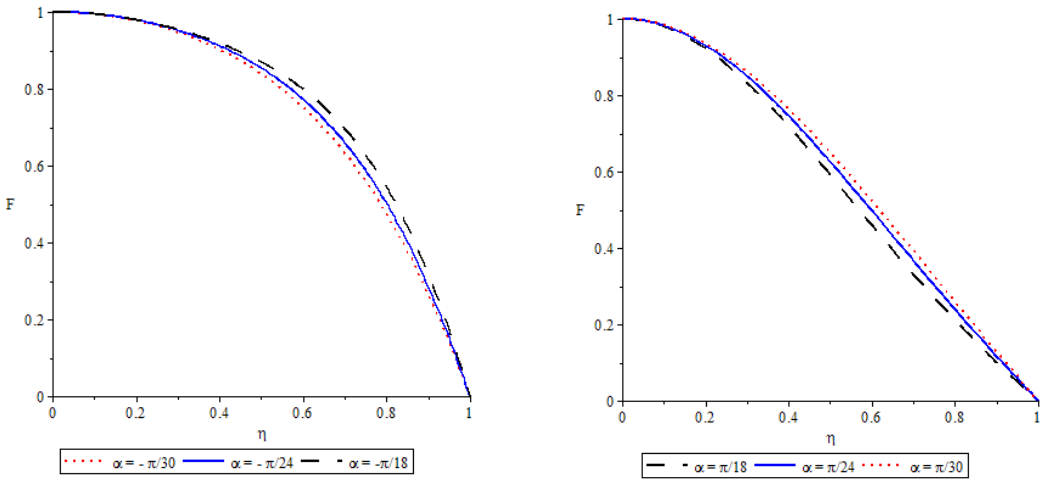

Fig.3a,b. Effect of semi angle on Velocity profile in case Re = 30, φ =0.1 and H=100 upper- converging channel, down- diverging channel.

In Fig.4 the effect of the magnetic field strength on the radial velocity is depicted. According to the figure, by changing the Hartmann number (or the strength of magnetic field) w can easily control the nanofluid flow and this has an important influence on the working system's performance evaluation results. Therefore, by increasing Hartman number (Lorentz force) the occurrence of back flow phenomenon in the diverging channel will be prevented.

Increasing the magnitude of Hartman number results in an increment in radial velocity. As it is mentioned, back flow is highly possible for large Reynolds numbers in case the angle between the rigid walls is positive. Hence, we can come to the conclusion that the transverse magnetic field reduces pressure gradient and opposes the transport phenomena. As by varying Hartman number, we can change the Lorentz force produced by inducing magnetic field on the electrically conductive fluid, and this increment in Lorentz force leads to more resistance to transport phenomena.

Solid volume fraction of the nanoparticles is another influential parameter. In Fig.5 we have shown the effect of solid volume fraction on velocity profiles in case the half-angle is positive channel (diverging channel). As it is depicted in Fig.5, by decreasing solid volume fraction number, the velocity will be decreased. It means that by increasing the nano additive concentration and improving the thermo-physical properties of the fluid, fluid elements can be more intensely accelerated.

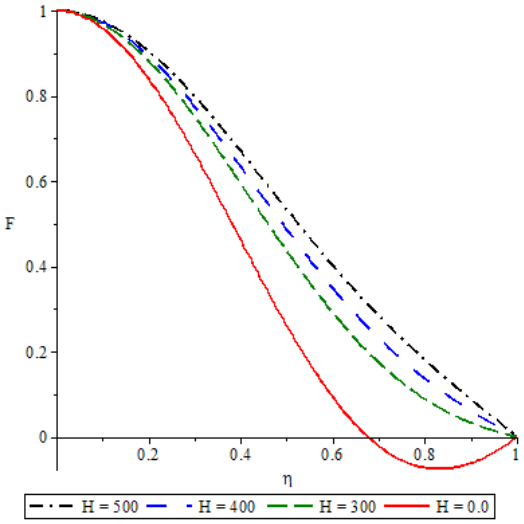

Fig.4. Effect of Hartman number on velocity profile in case$\alpha = Pi/24$, Re = 100, φ =0.0

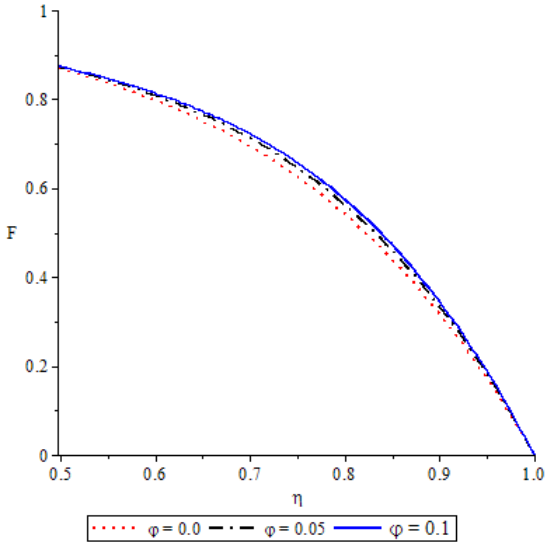

Fig.5. Effect of solid volume fraction number on velocity profiles in case $\alpha = -\frac{\pi}{18}$, Re = 40, H = 100

In Table.1, our results are compared to the results of recent study by Adel et al. In 2021 [27].

Table.1. Error Analysis (Adel et al.[27] vs. Current study) for case.A when Re=50, H=1000, and a = -10

x	Adel et al. [27]	Our results	Error
0.2	0.99763519	0.997629224	~ 0.1 %
0.4	0.98522918	0.985221386	~ 0.1 %
0.6	0.93520006	0.935192106	~ 0.1 %
0.8	0.73853168	0.738525188	~ 0.1 %

4.2. **Case. B:** In this section, we will present our achieved results.

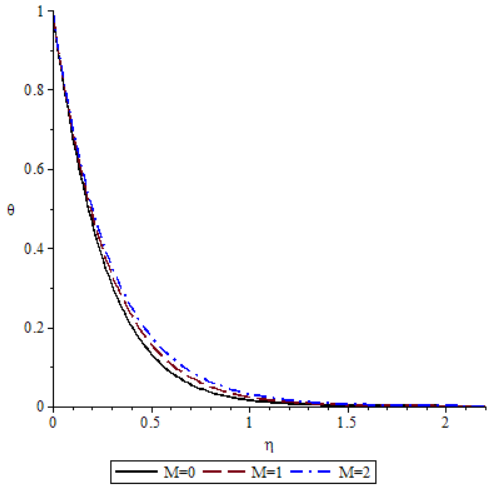

Fig. 6. Effect of Magnetic F on temperature profile

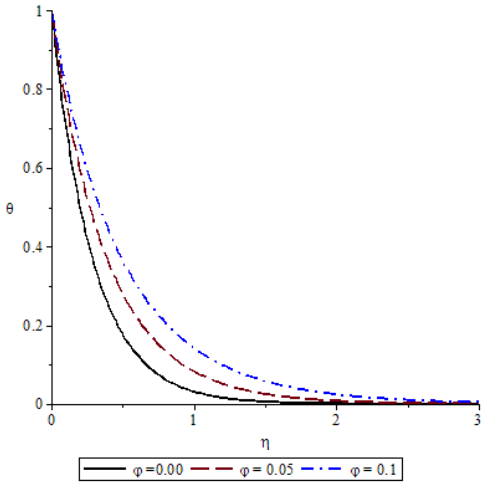

Fig. 7. Effect of Nanoparticle C on temperature profile

In Fig.6, the effect of external magnetic force on temperature profile is investigated. Fig.7 shows the effect of the volume fraction of copper nanoparticles on dimensionless temperature profiles. As can be seen from the figure, by increasing the volume fraction of copper nanoparticles in the base fluid, and because the thermophysical properties for the single-phase model are improved, we can obtain more thermal energy in the fluid.
Increasing the rate of heat transfer is one of the desirable phenomena in the industry, which can be achieved by adding nanoparticles to the base fluid, which is water here.
Figure 8 depicts the influence of the Eckert number on the temperature profile; as seen in this graph, the thickness of the thermal boundary layer increases as Ec increases. The impact of raising Ec values in the flow zone to increase temperature dispersion. The influence of viscous dissipation, which accounts for the heat energy stored in the fluid owing to frictional heating, is considered in this study. There is a magnification in order from figure to show the amount of difference better. It should be noted that to obtain Fig.8, other coefficients are considered s = 0.0, φ = 0.05 λ = 1.0, Pr = 6.2, M = 2.0, respectively.
Fig.9 shows the effect of a magnetic field on the velocity profile. The increase in velocity when the magnetic field reaches M = 1 from zero is greater than the increase in velocity when M reaches from one to two. This figure is obtained while φ = 0.05, Ec = 0.15, Pr= 6.2. By changing the Prandtl and Eckert number the velocity profile varies rapidly.

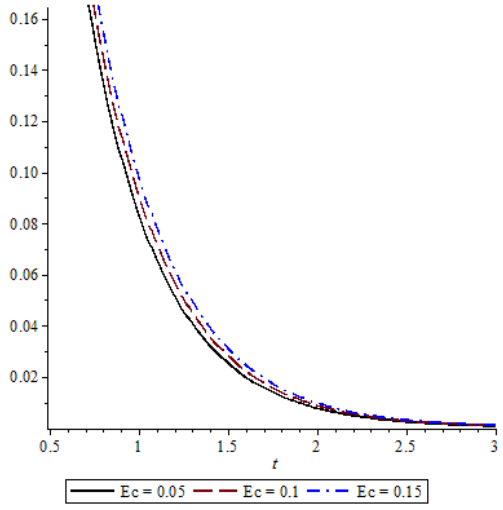

Fig. 8. Effect of Eckert number on temperature profile

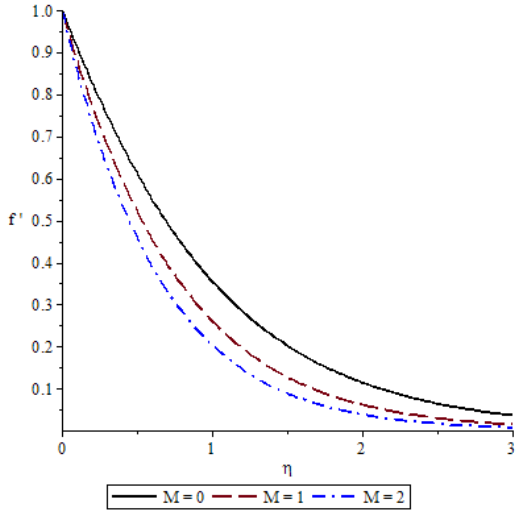

Fig. 9. Effect of Magnetic F on velocity profile

By introducing the following parameters, we can examine the error sensitivity and error analysis for the numerical solution obtained in this paper.

$$Nu_x Re_x{}^{0.5} = -\frac{k_{hnf}}{k_f}\theta'(0), C_f Re_x{}^{0.5} = \frac{f''(0)}{((1-\varphi_1)^{2.5}(1-\varphi_2)^{2.5})} \quad \textbf{(18)}$$

In Table.2, our results are compared to the results of study by Waini et al. [28].

Table.2. Error Analysis (Waini et al.[28] vs. Current study) for case.B.

φ_2	[28] $C_f Re_x^{0.5}$	Our results	[28] $Nu_x Re_x^{0.5}$	Our results	Error
0.005	-1.3287098	-1.3272937	1.961773	1.9616047	~0.1%
0.02	-1.409490	-1.4096591	1.989308	1.9891453	~0.1%
0.04	-1.520721	-1.5208630	2.026446	2.02628990	~0.1%
0.06	-1.634119	-1.6324060	2.064150	2.063997469	~0.1%

5. Validation

Case. A - ODES: Here, we also attempt to validate the achieved approximate results, so the ODEs subject to the BCs have been also solved analytically by HPM-Pade method. We have used MAPLE software for this purpose. In this section, the basic ideas of Homotopy Perturbation Method will be illustrated. Consider the following differential equation which is nonlinear:

$$A(F) - u(\eta) = 0, \quad \eta \in \Omega \tag{19}$$

Subject to the general boundary condition:

$$B\left(F, \frac{\partial F}{\partial n}\right) = 0, \quad \eta \in \Gamma \tag{20}$$

Here, A is a differential operator and B is a boundary operator while $u(\eta)$ is an analytical function, and the Γ is the Ω domain's boundary. According to the Homotopy Perturbation Method, the predefined operator A should be divided into two different parts: a. L (which is the linear part) b. N (which is the nonlinear part). So we can rewrite the Eq.(20):

$$L(F) + N(F) - u(\eta) = 0 \tag{21}$$

The structure of Homotopy Perturbation is defined as follows:

$$H(f,p) = (1-p)[L(f) - L(F_0)] + p[A(F) - u(\eta)] = 0 \tag{22}$$

Here, the embedding parameter $p \in [0,1]$ is introduced. Moreover, F_0 is an initial approximation that can satisfy the predetermined boundary condition. While the embedding parameter changes from zero to one, $f(\eta,p)$ can change from $F_0$to F_η:

$$f(\eta,p): \Omega \times [0,1] \to R \tag{23}$$

According to Eq.(22), we can obtain:

$$H(f,0) = L(f) - L(F_0) = 0 \tag{24}$$

By considering $f(\eta,p)$as:

$$f(\eta) = f_0(\eta) + pf_1(\eta) + p^2 f_2(\eta) + \cdots \tag{25}$$

Hence, the approximation is achieved:

$$F = f_0(\eta) + f_1(\eta) + f_2(\eta) + \cdots \tag{26}$$

Based on the HPM, the Homotopy form of our equation can be obtained as follows:

$$(1-p)\left(\frac{d^3f}{d\eta^3}-\frac{d^3F_0}{d\eta^3}\right) + p\left[\frac{d^3f}{d\eta^3}+2\,Re\,\alpha\left[(1-\varphi)^{2.5}\left(1-\varphi+\varphi\frac{\rho_s}{\rho_f}\right)\right]f\frac{df}{d\eta} + (4-(1-\varphi)^{1.25}H)\alpha^2\left(\frac{df}{d\eta}\right)\right]=0 \quad \textbf{(27)}$$

The proper linear operator will be later chosen to satisfy the boundary condition. The boundary conditions are:

$$f(0)=F(0)=1,\quad f'(0)=F'(0)=0,\quad f(1)=F(1)=0 \quad \textbf{(28)}$$

Inserting Eq.(25) into Eq.(27), and rearranging based on p-terms powers, the following set of equations will be achieved**:**

$$p^0:\frac{d^3f_0}{d\eta^3}-\frac{d^3F_0}{d\eta^3}=0 \quad \textbf{(29)}$$

$$p^1:\frac{d^3f_1}{d\eta^3}+(4-(1-\varphi)^{1.25}H)\alpha^2\left(\frac{df_0}{d\eta}\right)$$

We have considered A = $(1-\varphi)^{1.25}$ and B = $(1-\varphi)^{2.5}\left(1-\varphi+\varphi\frac{\rho_s}{\rho_f}\right)$ in order to simplify the solution of the Eq. (27) with boundary conditions. Solving the Eq.(27) yields:

$$f_0(\eta)=1-\eta^2 \quad \textbf{(30)}$$

$$f_1=-2\alpha\left(\frac{1}{60}Re\,B\,\eta^6+\frac{1}{24}(-4\alpha+\alpha HA-2\,Re\,B)\eta^4\right) + \frac{1}{2}\left(-\frac{4}{15}Re\,\alpha\,B-\frac{2}{3}\alpha^2+\frac{1}{6}\alpha^2AH\right)\eta^2$$

Thus, the solution is $F(\eta)=f_0(\eta)+f_1(\eta)+\cdots$. The ratio of polynomials constructed from the Taylor series expansions coefficient (of a known function) is referred to as Pade' approximate. The $\left[\frac{L}{M}\right]$Pade' approximates to a function $F(\eta)$ can be achieved by:

$$\left[\frac{L}{M}\right]=\frac{Z_L(\eta)}{Q_M(\eta)} \quad \textbf{(31)}$$

Here, $Z_L(\eta)$ is a polynomial of L degree and $Q_M(\eta)$ is a polynomial of M degree. The power series can be achieved (in terms of η):

$$F(\eta)=\sum_{i=0}^{\infty}a_i\eta^i \quad \textbf{(32)}$$

$$u(\eta)=\frac{Z_L(\eta)}{Q_M(\eta)}+O(\eta^{L+M+1}) \quad \textbf{(33)}$$

The coefficients of $Q_M(\eta)$and $Z_L(\eta)$ can be determined from Eq.(33). The denominator and numerator should be multiplied by a constant. By leaving $\left[\frac{L}{M}\right]$ unchanged, the normalization condition can be imposed:

$$Q_0(\eta) = q_0 = 1 \tag{34}$$

The prementioned polynomials $Z_L(\eta)$ and $Q_M(\eta)$ will be expanded in power series in terms of η of order L and M. Hence, we achieve:

$$Z_L(\eta) = z_0 + z_1\eta + z_2\eta^2 + \cdots + z_L\eta^L \tag{35}$$
$$Q_M(\eta) = 1 + q_1\eta + q_2\eta^2 + \cdots + q_M\eta^M$$

Using Eqs.(32), (35) in Eq(33), Eq.(33) can be rewritten in the notation of formal power series [29]:

$$\sum_{i=0}^{\infty} a_i\,\eta^i = \frac{z_0 + z_1\eta + z_2\eta^2 + \cdots + z_L\eta^L}{1 + q_1\eta + q_2\eta^2 + \cdots + q_M\eta^M} + O(\eta^{L+M+1}) \tag{36}$$

By cross multiplication of Eq.(35), and from Eq.(36), the next set of linear equations can be obtained:

$$\begin{cases} a_0 = z_0 \\ a_1 + a_0 q_1 = z_1 \\ . \\ . \\ a_L + a_{L-1}q_1 + \cdots + a_0 q_L = z_L \end{cases} \tag{37}$$

And,

$$\begin{cases} a_{L+1} + a_L q_1 + \cdots + a_{L-M+1} q_M = 0 \\ a_{L+2} + a_{L+1} q_1 + \cdots + a_{L-M+2} q_M = 0 \\ . \\ . \\ a_{L+M} + a_{L+M-1} q_1 + \cdots + a_L q_M = 0 \end{cases} \tag{38}$$

From Eq.(38), we get q_i, $1 < i < M$. As the values of$q_1, q_2, \cdots, q_M$ are all known, the formula for the unknown quantities $z_1, z_2, \cdots, z_L$ will be given by Eq.(37). The diagonal approximants like [4/4], [5/5], [6/6] are more accurate in comparison with nondiagonal approximates. The diagonal approximates can be calculated by built-in utilities of Maple. It should be noted that MAPLE software is used to achieve the diagonal pade' approximants. The effect of one of the influential parameters (Reynolds number) on velocity profile in case H=40 and φ =0.1 is shown in Fig.10 As it can be illustrated in Fig.10 , by increasing the Reynolds number, the velocity will be increased uniformly. We have also presented a comparison between numerical results and approximate analytical solution obtained from HPM-pade' method in the same figure. The achieved results have a very good agreement with analytical solutions, according to the figure.

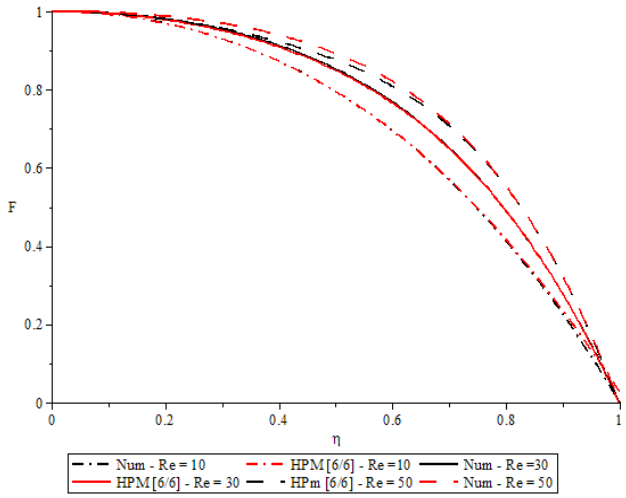

Fig. 10. Effect of Reynolds number on Velocity profile: H=40, φ =0.1 (Red: Pade'[6/6], Black: RK4)

Case. B - PDES: To validate our results, the code developed by Vakilipour et al. [30] has been used. In Fig.11, we have presented the data obtained from the similarity solution (ODE) and the Vakilipour et al code (CFD). Fig.12 shows the effect of nanoparticles solid volume fraction increment on the temperature profile, using Runge Kutta (ODE) and CFD solution. By comparing the results obtained by the CFD method with our obtained data (ODE), we can ensure the validity of the archived results.

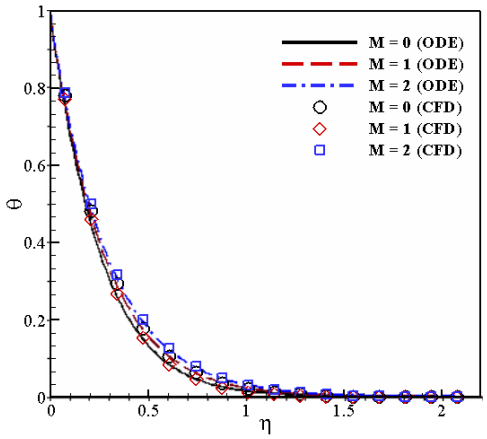

Fig.11. Effect of M on temperature profile when $s = 0.0, \lambda = 1\ Ec = 0.05, Pr = 6.2, \varphi = 0.0$

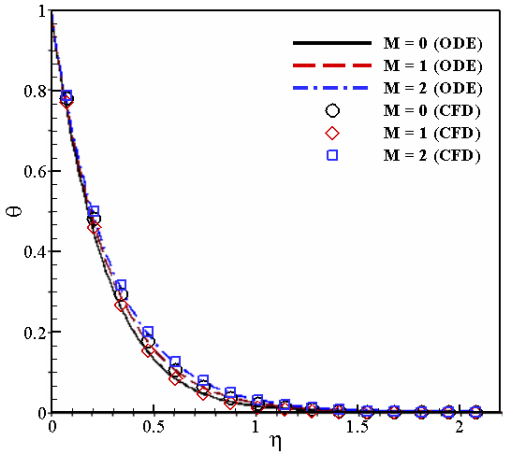

Fig.12. Effect of M on temperature profile when $s = 0.0, \lambda = 1\ Ec = 0.05, Pr = 6.2, M = 2.0$

6. Conclusions

This paper is devoted to the numerical study of magnetohydrodynamic (MHD) problems on a flow of a conducting nanofluid over an inclined plate as well as MHD nanofluid flow between two inclined plates. Two different approaches are employed to investigate the flow and heat transfer characteristic of a viscous, incompressible and electrically conducting nanofluid. The fourth order Runge Kutta method has been used for achieving the results for both of the cases. To validate the results, a pressure-based finite volume-based solver is also utilized. The chosen semi analytical approach for validation of the results is Homotopy Perturbation Method-Pade'. The effects of different parameters, such as Hartmann number or external magnetic field strength, nanoparticles solid volume fraction, and etc. on velocity and temperature profiles have been studied. The achieved results are compared with those of numerical solution in several numerical cases. In this work, Maple 17 software as a powerful mathematical tool for analytical studies has been exploited and for analytical investigation firstly, a local similarity solution for the transformed governing equations is obtained. The reduced ordinary differential equations are solved once the governing partial differential equations and boundary conditions are transformed into a dimensionless form. We showed the thickness of thermal boundary layer decreases with increment in solid volume fraction of nanofluid due to higher heat transfer rate. For the first case, a steady, laminar nanofluid flow through a converging-diverging channel is investigated in this article. The beginning part of this article was concerned with to the consideration of MHD flow in a wedge-shaped channel of water-copper nanofluid. For validation of the numerical results, an analytical solution for MHD flows of copper water nanofluid between two nonparallel plates is presented. For both cases, a similarity transform reduces the Navier– Stokes and energy equations to a set of non-linear ordinary differential equations. We solved the equations then analytically by means of the Runge Kutta method. Close agreement of the numerical and analytical results assures us about the accuracy of HPM-Pade'. The effects of key parameters on are studied carefully through some plots. For the second part a pressure-based finite volume-based solver is used.

References

[1] Muneeshwaran, M., *et al*., Role of hybrid-nanofluid in heat transfer enhancement – A review, *International Communications in Heat and Mass Transfer, 125* (2021), 105341.

[2] Sheikholeslami, M., Farshad, S.A., Investigation of Solar Collector System with Turbulator Considering Hybrid Nanoparticles, *Renewable Energy, 171* (2021), pp. 1128-1158.

[3] Zhang, D., *et al*., Heat transfer and flow visualization of pulsating heat pipe with silica nanofluid: An experimental study, *International Journal of Heat and Mass Transfer, 183* (2022), 122100.

[4] Olabi, A.G., *et al*., Geometrical effect coupled with nanofluid on heat transfer enhancement in heat exchangers, *International Journal of Thermofluids 10* (2021), 100072.

[5] Wiriyasart, S., *et al.*, Heat transfer enhancement of thermoelectric cooling module with nanofluid and ferrofluid as base fluids, *Case Studies in Thermal Engineering 24* (2021), 100877.

[6] Azimi, M., Riazi, R., MagnetoHydroDynamic GO-water Nanofluid Flow and Heat Transfer between Two Parallel Disks, *Thermal Science, 22* (2018), 1, pp.383-390.

[7] Azimi, M., Mozaffari, A., Heat Transfer Analysis of Unsteady Graphene Oxide Nanofluid Flow Using a Fuzzy Identifier Evolved by Genetically Encoded Mutable Smart Bee Algorithm, *Engineering Science and Technology, an International Journal, 18* (2015), 1, pp.106-123.

[8] Ali, A., Shehzadi, *et al*., Heat and Mass Transfer Analysis of 3D Maxwell Nanofluid Over an Exponentially Stretching Surface, *Physica Scripta, 94* (2019), 6, p.065206.

[9] Sheikholeslami, M., Bhatti, M. Active Method for Nanofluid Heat Transfer Enhancement by Means of EHD, *International Journal of Heat and Mass Transfer, 109* (2017), pp.115-122.

[10] Nilsson, S., *Feasibility study of magnetic flow meters for molten salt reactors*, Thesis, 2020.

[11] Kumbinarasaiah, S., Raghunatha., K. R., Numerical solution of the Jeffery–Hamel flow through the wavelet technique, *Heat Transfer, 51* (2022).

[12] Qayyum, M., Oscar, I., Exploration of Unsteady Squeezing Flow Through Least Squares Homotopy Perturbation Method, *Journal of Mathematics* (2021).

[13] Azimi, M., Riazi, R., MHD Unsteady Go-Water-Squeezing Nanofluid Flow-Heat and Mass Transfer Between Two Infinite Parallel Moving Plates: Analytical Investigation, *Sadhana, 42* (2017), 3, pp.1-7.

[14] Azimi, M., Riazi, R., Flow and Heat Transfer of MHD Graphene Oxide-Water Nanofluid Between Two Non-parallel Walls, *Thermal Science, 21* (2017), 5, pp. 2095-2104

[15] Chaich, Z., *et al.,* Thermodynamic Analysis of Viscoelastic Fluid in a Porous Meduim with Prescribed Wall Heat Flux over Stretching Sheet Subjected to a Tansitive Magnetic Field, *Thermal Science,* 23 (2019), 1, pp. 219-231.

[16] Dadheech, Prvaeen Kumar, *et al.,* Transportation of Al2O3-SiO2-TiO2 Modified Nanofluid Over an Exponentially Stretching Surface with Inclined Magnetohydrodynamic., *Thermal Science, 25* (2021), pp.279-285.

[17] Shen, Bingyu, *et al.,* Bioconvection Heat Transfer of a Nanofluid Over a Stretching Sheet with Velocity Slip and Temperature Jump, *Thermal Science, 21* 2017, pp.2347-2356.

[18] Awad, Mohamed M., Comments on "Magnetohydrodynamic flow of nanofluid over permeable stretching sheet with convective boundary conditions", *Thermal Science, 24* (2020), 5A, p.3047.

[19] Al-Mamun, *et al.,* Numerical Simulation of Periodic MHD Casson Nanofluid Flow Through Porous Stretching Sheet, *SN Applied Sciences, 3* (2021), 2, pp. 1-14.

[20] Khashi'ie, N.S., *et al.,* Three-Dimensional Hybrid Nanofluid Flow and Heat Transfer Past a Permeable Stretching/Shrinking Sheet with Velocity Slip and Convective Condition, *Chinese Journal of Physics, 66* (2020), pp. 157-171.

[21] Wahid, N.S., Arifin, N.M., Khashi'ie, N.S., Pop, I.: Hybrid nanofluid slip flow over an exponentially stretching/shrinking permeable sheet with heat generation. Mathematics 9(1), 30 (2021).

[22] Ali, L., et.al., Analysis of magnetic properties of nano-particles due to a magnetic dipole in micropolar fluid flow over a stretching sheet. Coatings 10(2), 170 (2020).

[23] Hazarika, S., et.al., Investigation of nanoparticles Cu, Ag and Fe3O4 on thermophoresis and viscous dissipation of MHD nanofluid over a stretching sheet in a porous regime: A numerical modelling. Mathematics and Computers in Simulation 182, 819–837 (2021).

[24] Hayat, T., et.al., Impact of induced magnetic field on second-grade nanofluid flow past a convectively heated stretching sheet. Applied Nanoscience 10(8), 3001–3009 (2020).

[25] Dennis, S., et.al., Flow along a diverging channel. Journal of Fluid Mechanics 336, 183–202 (1997).

[26] Nourazar, S., et.al., On the expedient solution of the magneto-hydrodynamic jeffery-hamel flow of casson fluid. Scientific reports 8(1), 1–16 (2018).

[27] Adel, W., et al., Numerical Approach for Simulating the Nonlinear MHD Jeffery–Hamel Flow Problem, *International Journal of Applied and Computational Mathematics 74* (2021).

[28] Waini, I., et.al, Unsteady Flow and Heat Transfer Past a Stretching/Shrinking Sheet in a Hybrid Nanofluid, *International Journal of Heat and Mass Transfer, 136* (2019), pp. 288-297.

[29] Varun Kumar, R. S., et al. Effect of electromagnetic field on the thermal performance of longitudinal trapezoidal porous fin using DTM–Pade approximant, *Heat Transfer* (2022).

[30] S. Vakilipour, et.al., Developing a physical influence upwind scheme for pressurebased cell-centered finite volume methods, *International Journal for Numerical Methods in Fluids 89* (2019) , 1, pp.43-70.

Submitted: 29.01.2022

Revised: 20.02.2022

Accepted: 26.02.2022